Journal of Engineering Sciences, Assiut University, Vol. 40, No. 3, pp. 849-866, May 2012

FAULT DURATION FOR VOLTAGE INSTABILITY AND VOLTAGE COLLAPSE INITIATION AS INFLUENCED BY GENERATOR VOLTAGE MAGNITUDES (GVM)

Youssef A. Mobarak
Electrical Engineering Department, Faculty of Energy Engineering, South Valley University, Aswan, Egypt

(Received January 24, 2012 Accepted March 8, 2012)

The occurrence of voltage instabilities or voltage collapses depend on the duration of the persistence of the fault and on the type of fault, some faults lead to voltage instabilities, others lead to voltage collapse. Evaluation of fault durations causing occurrence of voltage instabilities or collapse is the main goal of this paper. The effect of the generators terminal voltages magnitudes (GVM) on fault duration which causes voltage instability initiation is investigated. The fault which leads to voltage instability is found to be three-phase short-circuits at certain load bus and cleared without any variation in the transmission system elements, i.e. the post-fault network conditions will be the same as its pre-fault conditions. Also, this paper searches for the effect of GVM on fault duration for voltage collapse. Where, some line opening in the studied system can be lead to occur the phenomena of voltage collapse initiation.

KEYWORDS: *Voltage Instability, Voltage Collapse, GVM.*

1. INTRODUCTION

Voltage instability concerns voltage fluctuations around nominal values. These fluctuations are either periodic or non periodic. The main factor causing voltage instability is the inability of the power system to meet the demand for service power. The heart of the problem is usually the voltage drop that occurs when active and reactive power flow through the series inductive reactances of the transmission network [1-5]. A criterion for voltage stability is that, at a given operating condition for every bus in the system, the bus voltage magnitude increases as the reactive power injection at the same bus is increased. A system is unstable if for at least one bus in the system, the bus voltage magnitude decreases as the reactive power injection at the same bus is increased. In other words, a system is voltage unstable if V-Q sensitivity is negative for at least one bus [5, 10].

Voltage collapse is a rapid progressive voltage fall and settling at certain value defined by system parameters, it is more complex than simple voltage instability and usually the result of a sequence of events accompany voltage instability leading to a low voltage profile in a significant part of the power system lasting long periods [11-16]. Voltage stability is the ability of a power system to maintain steady acceptable voltages at all buses in the system under normal operating conditions and after being subjected to a disturbance. A system enters a state of voltage instability when disturbance such as increase in load demand, or change in system condition causes a progressive and uncontrolled drop in voltage [17-21]. This paper studies the effect of

the GVM (of all generating units) on fault duration causing voltage instability, when a 3-phase short circuit occurs at certain load bus, with different types of loads. Also, studies the effect of the all GVM on the fault duration causing voltage collapse, when opening line between two buses in the studied system, with different types of loads [22-25].

2. POWER SYSTEM MODEL REPRESENTATION

The power system considered consisting of *n* synchronous generators feeding through a transmission network, a number of loads. The system motion using one-axis generator model, under a disturbance, the following set of differential equations described for each generator [6]:

$$\dot{\delta}_i = 2\pi f_{0i}\ \omega_i \tag{1}$$

$$\dot{\omega}_i = (P_{mi} - P_{ei} - D_i\omega_i)/2H_i \tag{2}$$

$$\dot{E}'_{qi} = (E_{fdi} - E'_{qi} - (X_{di} - X'_{di})I_{di})/T'_{doi} \tag{3}$$

Where: δ, f_0, ω, H, D, and E'_{qi} are the rotor angle, initial frequency, speed deviation, inertia constant, mechanical damping coefficient, and the q-axis voltage component, respectively. P_m, P_e, E_{fd}, I_d, and T'_{d0} are the generator input mechanical power, output electrical power, excitation voltage, d-axis current component, and d-axis transient open-circuit time constant, respectively. Finally, X_d and X'_d are the d-axis and transient d-axis reactance's. Note that, P_e is computed as:

$$P_{ei} = E'_{qi}I_{qi} + E'_{di}I_{di} \tag{4}$$

Where, E'_d is the d-axis component of the voltage E', and I_q is the q-axis component of the generator current, which is given as:

$$I_i = (E'_i - V_i)/(jX'_{di}) \tag{5}$$

Where, E' is the voltage behind the reactance X'_d, and V is the generator terminal voltage.

In this paper, we concerned with the study of the quasi static loads which it consists of heating and lighting equipments. Also, three quasi static models are used for induction motor load representation. The commonly used representations of static loads are either constant impedance to ground, constant current and constant real and reactive power [1, 2]. These load models are given in the following, where P_L, Q_L and V_L are the load active power, reactive power, and bus voltage, respectively (their initial values are P_{Lo}, Q_{Lo} and V_{Lo}).

Constant Impedance Model (C.Z.):

$$P = P_0\left(\frac{V}{V_0}\right)^2 \ , \ Q = Q_0\left(\frac{V}{V_0}\right)^2 \tag{6}$$

Constant Current Model (C.I.):

$$P = P_0\left(\frac{V}{V_0}\right) \ , \ Q = Q_0\left(\frac{V}{V_0}\right) \tag{7}$$

Constant Power Model (C.P.):

$$P = P_0\left(\frac{V}{V_0}\right)^0 \ , \ Q = Q_0\left(\frac{V}{V_0}\right)^0 \tag{8}$$

Three models are used for induction motor load, and the active and reactive power has expressed by the 4th order polynomials representation [9]:
Induction motors with constant mechanical loads torque (T=Const.):

$$P=0.275+8.79V-23.27V^2+23.233V^3-8.017V^4$$

$$Q=-16.11+92.94V-179.72V^2+148.56V^3-44.67V^4 \tag{9}$$

Induction motors with mechanical load torque proportional to speed (T α ω):

$$P=-33+161.67V-286.033V^2+233.033V^3-64.67V^4$$

$$Q=48.83-175.67V+237.5V^2-142.22V^3+32.56V^4 \tag{10}$$

Induction motors with mechanical load torque proportional to square of speed (T α ω^2):

$$P= 9.233-81.567V+309.9V^2-598.5V^3+627.967V^4-342V^5+75.967V^6$$

$$Q= 46.739-53.15V+1721.67V^2-325V^3+3488.704V^4-1900V^5+422.037V^6 \tag{11}$$

The interrelation of the system elements is shown in figure (1). The three systems solution is the dynamic simulation program, the network reduction program and the load flow program with loads represented by polynomial models. They should be used in sequence to solve the system equations. The system performance is determined by solving the machine mathematical models together with the constraints imposed by the network. The non-linear machine models are solved numerically using the appropriate integration technique. For network having total *N* buses the calculated voltage at any bus is described by the following nonlinear equations:

$$E_K = \frac{1}{Y_{KK}}\left(\frac{P_K - jQ_K}{E_K^*} - \sum_{\substack{j=1 \\ j\neq K}}^{N} Y_{Kj}E_j\right) \tag{12}$$

With: $K=1, 2, \ldots..N$, and $K \neq S$, where S means slack bus, E_K is voltage at node K, E_K^* is E_K conjugate, Y_{KK} Self admittance at node K, Y_{Kj} The mutual admittance between node K and node j, E_j Voltage at node j, P_K, Q_K Scheduled real and reactive power entering the system at bus K.

$$P_k = P_{ko}\,(a_0 + a_1S + a_2S^2 + a_3S^3 + a_4S^4 + \ldots\ldots\ldots\ldots)$$

$$Q_k = Q_{ko}(b_0 + b_1S + b_2S^2 + b_3S^3 + b_4S^4 + \ldots\ldots\ldots\ldots) \tag{13}$$

Where: $S=V/V_0$, and the active and reactive power components at the slack bus are then computed as:

$$P_S - jQ_S = \sum_{\substack{K=1 \\ K \neq S}}^{N} P_{SK} - jQ_{SK}$$
$$P_S - jQ_S = \sum_{\substack{K=1 \\ K \neq S}}^{N} E_S^* * (E_S - E_K) * Y_{SK} \quad (14)$$

Where: $P_S - jQ_S$ Load at the slack bus, Y_{SK} Mutual admittance between *S* and *K* nodes, and E_S Voltage at the slack bus.

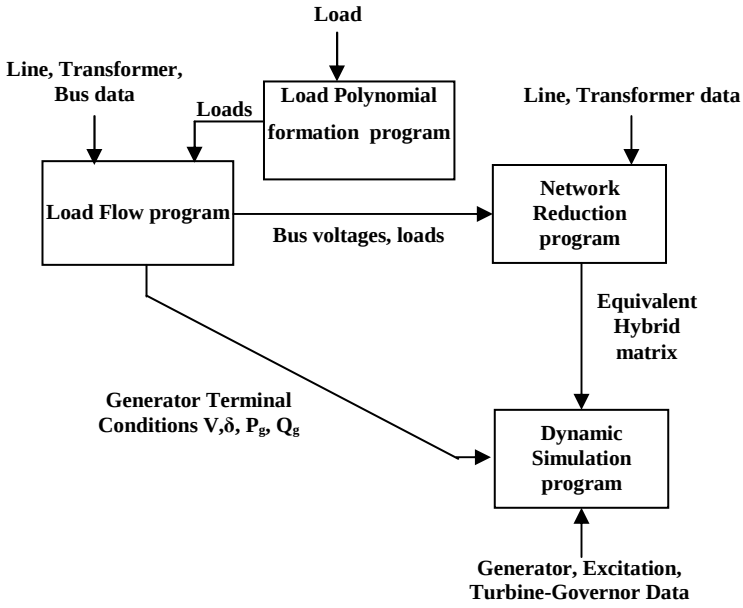

Fig. (1) Data requirements of power system simulation program and its support

From all the dynamic models involved in this type of simulation, the electric alternators is the one requiring more calculations since the rest of the dynamic components are given by a block diagram, in the initial condition calculations are made by simply setting to zero any term containing a derivative term [14]. Using the phasor diagram shown in figure (2) the initial condition for the synchronous generator can be calculated as follows: At the terminal side of every alternator, the known variables given by a load-flow study, are: Terminal voltage $\bar{V}_a$, and Generated active power *P*, and reactive power *Q*. Knowing these variables, it is easy to calculate the armature current of every unit and the corresponding power factor by:

$$\bar{I}_a = \left(\frac{P + jQ}{\bar{V}_a} \right)^* \quad (15)$$

Where: $\overline{I_a}$ is the armature current phasor, and Resolve $\overline{I_a}$ into components with $\overline{V_a}$ as a reference: $I_r = I_a \cos\phi, I_x = -I_a \sin\phi$, and the phasor $\overline{E}_{qa}$ in figure (2), is given by:

$$\overline{E}_{qa} = \overline{V_a} + (r + jx_q)\overline{I}_a = V_a + (I_r + jI_x)(r + jx_q) = (V_a - x_q I_x + rI_r) + j(x_q I_r + rI_x) \quad (16)$$

Then the angle $(\delta - \beta)$ is given by:

$$\delta - \beta = \gamma = \arctan(I_x r + I_r x_q)/(V_a - x_q I_x + rI_r) \quad (17)$$

where angle δ is the position of the rotor.
Then, calculate the terminal voltage d-q components:

$$V_d = -V_a \sin(\delta - \beta), V_q = V_a \cos(\delta - \beta) \quad (18)$$

Also, the armature current d-q components:

$$I_d = -I_a \sin(\delta - \beta + \phi), I_q = I_a \cos(\delta - \beta + \phi) \quad (19)$$

The field voltage of the machine from the stator side can be calculated by: $E = V_q + rI_q - x_d I_d = E_{FD}$. The initial position of the rotor is calculated by: $\delta = \gamma + \beta$. Calculate the initial value of the state variable of the alternator model using the quantities just calculated. Repeat the whole process for all the electric alternators present.

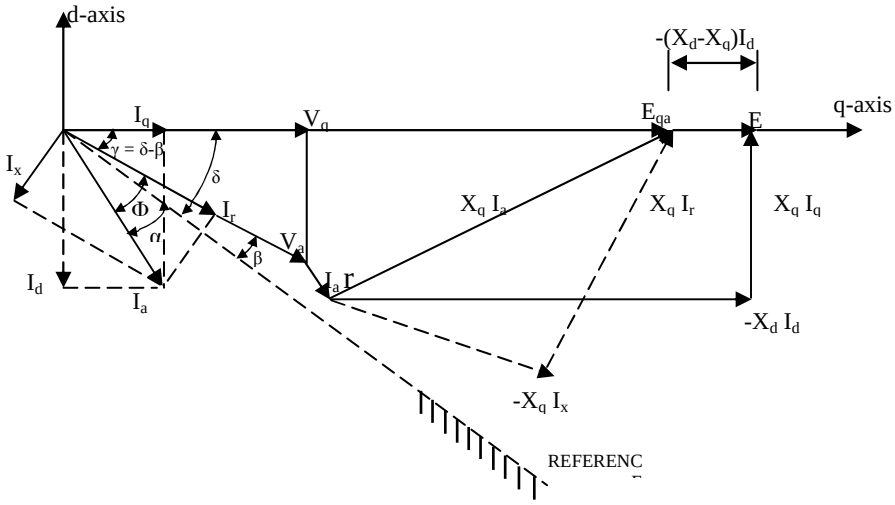

Fig. (2) Phasor diagram of alternator initial condition.

Once the bus admittance matrix representing the network has been built and its entries organized as generator nodes, non-linear load nodes and other nodes, it is necessary to eliminate those nodes with zero current injections. The procedure to obtain the reduced network is as follows:

Assume the Y_{BUS} matrix is partitioned in the following way:

$$\begin{bmatrix} I_G \\ I_L \\ 0 \end{bmatrix} = \begin{bmatrix} Y_{GG} & Y_{GL} & Y_{GR} \\ Y_{LG} & Y_{LL} & Y_{LR} \\ Y_{RG} & Y_{RL} & Y_{RR} \end{bmatrix} \begin{bmatrix} V_G \\ V_L \\ V_R \end{bmatrix} \tag{20}$$

Where: *G* means generator nodes, *L* means non-linear load nodes, *R* means remaining nodes. Eliminate the remaining nodes by successive elimination procedure:

$$\begin{bmatrix} I_G \\ I_L \end{bmatrix} = \begin{bmatrix} Y'_{GG} & Y'_{GL} \\ Y'_{LG} & Y'_{LL} \end{bmatrix} \begin{bmatrix} V_G \\ V_L \end{bmatrix} \tag{21}$$

Where: $Y'_{GG} = Y_{GG} - Y_{GR} Y_{RR}^{-1} Y_{RG}$, $Y'_{GL} = Y_{GL} - Y_{GR} Y_{RR}^{-1} Y_{RL}$,
$Y'_{LG} = Y_{LG} - Y_{LR} Y_{RR}^{-1} Y_{RG}$, and $Y'_{LL} = Y_{LL} - Y_{LR} Y_{RR}^{-1} Y_{RL}$

After adding the internal impedance of each generator to new admittance matrix, the equation (21) becomes re-arranged as follows:

$$\begin{bmatrix} I_G \\ I_L \end{bmatrix} = \begin{bmatrix} Y''_{GG} & Y'_{GL} \\ Y'_{LG} & Y'_{LL} \end{bmatrix} \begin{bmatrix} E'_G \\ V_L \end{bmatrix} \tag{22}$$

Where just Y'_{GG} change to Y''_{GG}, and E'_G means the voltage behind the transient reactance. The equation (22) can be re-arranged as follows, this is because the initial load current at load buses are known, and it is used to determine the load voltage at load buses respectively at the next step.

$$\begin{bmatrix} I_G \\ V_L \end{bmatrix} = \begin{bmatrix} Y^*_{GG} & K_{GL} \\ H_{LG} & Z_{LL} \end{bmatrix} \begin{bmatrix} E'_G \\ I_L \end{bmatrix} \tag{23}$$

Where: Y^*_{GG} New admittance matrix, K_{GL}, H_{LG} Non-dimensional matrices, Z_{LL} Load impedance matrix. The equivalent matrix for the entire network is represented by the single line diagram of power system operating at the nominal loading condition is found as:

$$\text{Where: } I_L = \frac{P_L - jQ_L}{V_L^*} \tag{24}$$

$$P_L = P_{ko}\,(a_0 + a_1 S_L + a_2 S_L^2 + a_3 S_L^3 + a_4 S_L^4 + \ldots\ldots\ldots),$$
$$Q_L = Q_{ko}(b_0 + b_1 S_L + b_2 S_L^2 + b_3 S_L^3 + b_4 S_L^4 + \ldots\ldots\ldots) \tag{25}$$

3. STUDIED SYSTEM

The power system used for digital simulation consists of multi-machine nine-bus system developed by Western States Coordinating Council (WSCC) in United States. A single line impedance diagram of the system is shown in fig. (3). Where the system is basically composed of three generating units and three loads, load A, load B, and load C are located at buses # 4, # 5, and # 6, respectively. Unit one is hydroelectric, while units two and three are steam driven generators.

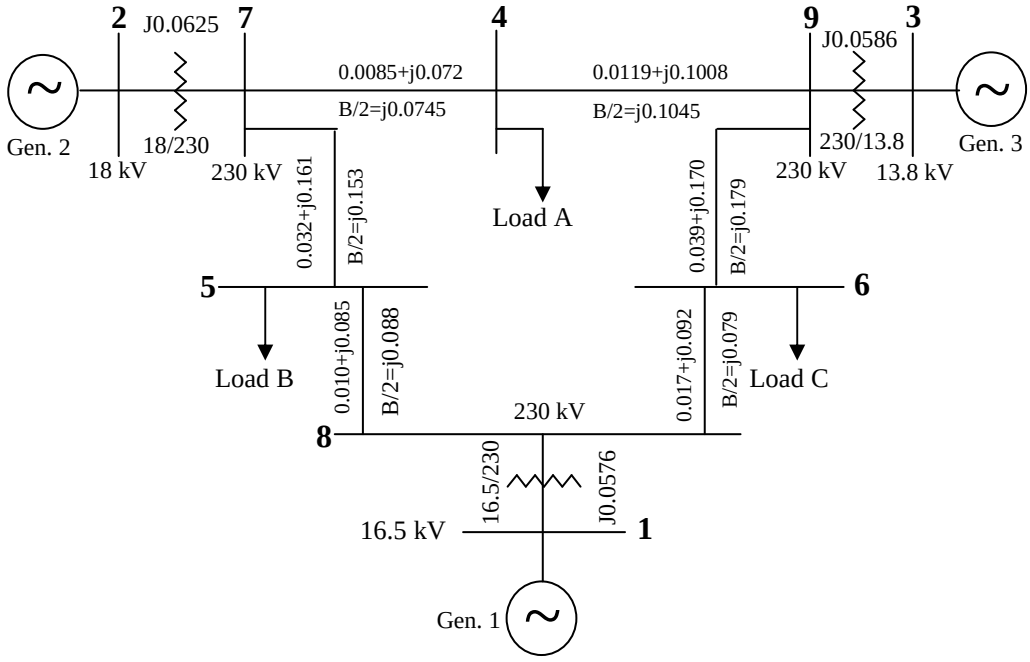

Fig. (3) Studied system single line diagram

4. RESULTS AND DUSCUSSIONS

4.1 Effect of suddenly increasing of the GVM on the duration period for voltage instability:

Figure (4) indicate the fault duration which cause voltage instability when all GVM are adjusted successively to (0.80, 0.85, 0.90, 0.95, 1.00, 1.05, 1.10, 1.15, and 1.20) p.u., Those voltages are applied when the loads are considered (constant impedance load, constant current load, constant power load) at all load buses, and induction motor with three shaft mechanical loads (I.M. load (T=const.), I.M. load (Tα ω) and I.M. load (Tα ω^2)) at load bus (4) while the loads at buses (5) and (6) having constant impedance loads, respectively. The fault duration which cause voltage instability increases by increasing GVM for each type of loads such as constant impedance load, constant current load, and constant power load at all load buses, as shown in figure 4 (a). The fault duration which cause voltage instability increases by increasing GVM for each type of induction motor loads such as I.M. load (T=constant), I.M. load (T α ω), and I.M. load (T α ω^2) at load bus (4) with the load at load buses (5) and (6) are constant impedance loads, as shown in figure 4 (b).

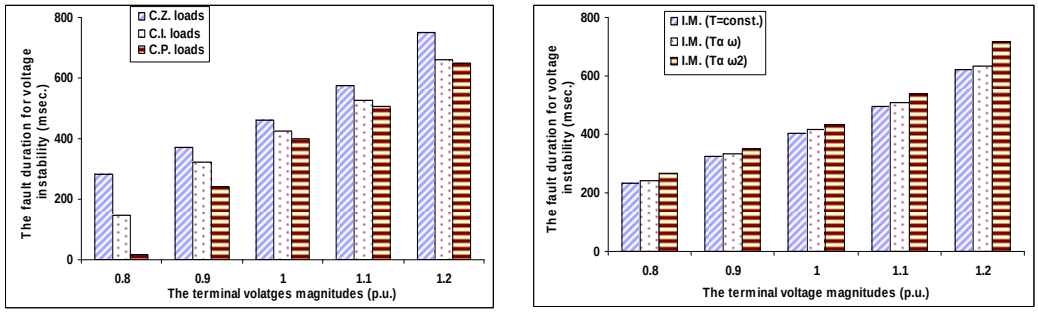

(a) when loads are connected at all load buses (b) when I.M. loads are connected at load bus (4)

Fig. (4) Effect of varying GVM on the fault duration for voltage instability, when a 3-phase short-circuit occurs at node (4)

4.2 Voltage stability limits due to opening the line with the GVM varies by (0.8 to 1.2) p.u.:

Figure (5) indicate the fault duration required for voltage collapse when opening the transmission line connected between two nodes (5) and node (7) at t=1 sec., with the GVM varies such as (0.80, 0.85, 0.90, 0.95, 1.00, 1.05, 1.10, 1.15, and 1.20) p.u., these varies are applied when the loads are (constant impedance load, constant current load, constant power load) at all load buses, and induction motor with three shaft mechanical loads (I.M. load (T=const.), I.M. load (Tα ω) and I.M. load (Tα ω^2)) at load bus (4) with the load at load buses (5) and (6) are constant impedance loads. It can be noted that, the fault duration which cause voltage collapse increases by increasing the GVM for each type of loads such as (constant impedance load, constant current load and constant power load) at all load buses, as shown in figure 5 (a). Also, the fault duration which cause voltage collapse initiation increases by increasing the GVM for each type of induction motor loads such as I.M. load (T=constant), I.M. load (T α ω) and I.M. load (T α ω^2) at load bus (4) with the load at load buses (5) and (6) are constant impedance loads, as shown in figure 5 (b).

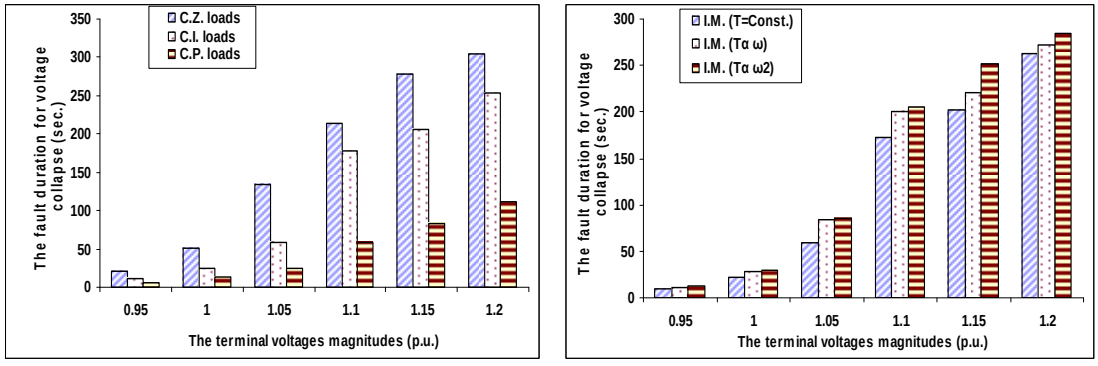

(a) Loads are connected at all load buses (b) IM loads are connected at load bus # 4

Fig. (5) Effect of varying the GVM on the fault duration for voltage collapse, when opening the line between buses # 5 and # 7

4.3 Time response for loads voltages with the GVM of generating units are (0.9p.u., and 1.1p.u.):

The time response for load buses voltages at load buses with two GVM 0.9 p.u., and 1.1 p.u., for all loads are considered as constant impedance, and constant power loads. Also at load bus (4) studied I.M. load (T=const.), and I.M. load ($T \alpha \omega^2$) with loads at (5), and (6) are constant impedance loads. A three-phase short-circuit is applied at node (4) and recovered without any changing in network configuration. Figure (6) indicates that, the time response of load buses voltages with the GVM of generating units are (0.9 p.u., and 1.1 p.u.) with the loads at all load buses are constant impedance loads. With all GVM of 0.9 p.u., a fault duration of 371 msec. turns the system voltage to be stable and a fault duration of 372 msec. makes the system to start to be unstable, as shown in figure 6 (a, b) respectively. For GVM of 1.1 p.u. those values are 575 msec. and 576 msec. respectively, also as shown in figure 5 (c, d) respectively. Also, figure 6 (e, f, g and h) depicts the same above results when all loads are represented by constant power loads, less fault duration periods are depicted, in the two cases, than those with constant impedance loads.

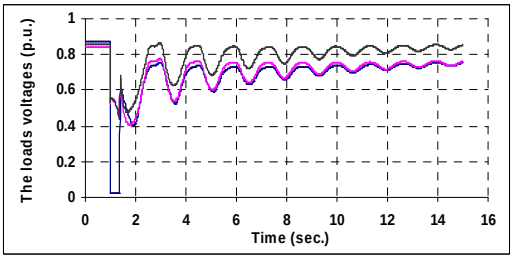

(a) V_S=0.9pu, CZ Loads, and T_C=371msec

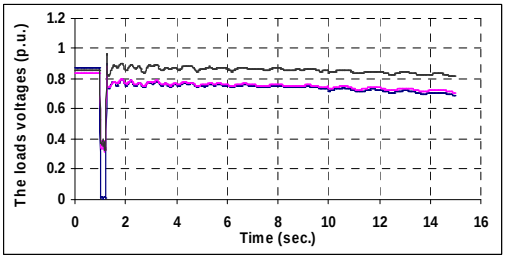

(e) V_S=0.9pu, CP Loads, and T_C=239msec

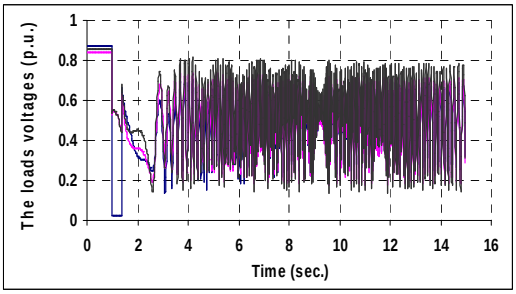

(b) V_S=0.9pu, CZ Loads, and T_C=372msec

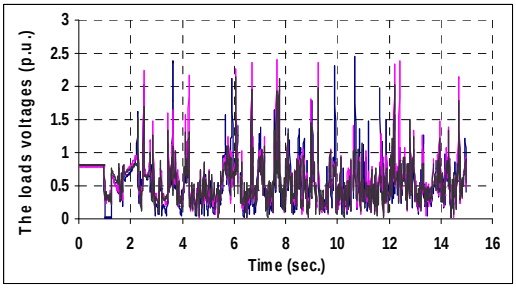

(f) V_S=0.9pu, CP Loads, and T_C=240 msec

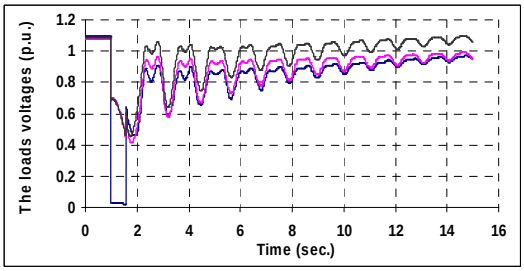

(c) V_S=1.1pu, CZ Loads, and T_C=575msec

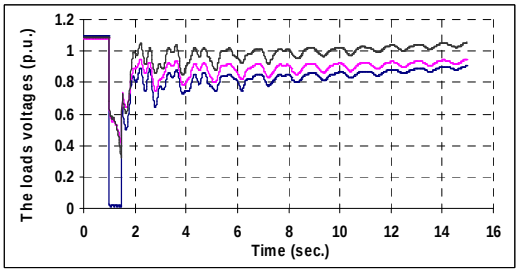

(g) V_S=1.1pu, CP Loads, and T_C= 504msec

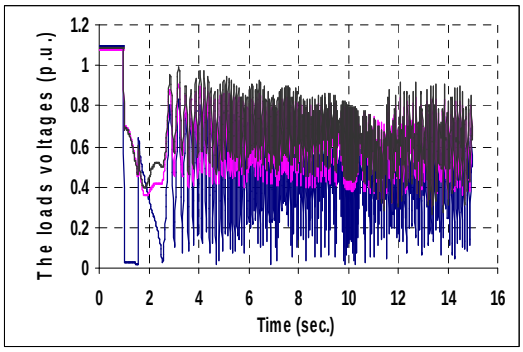

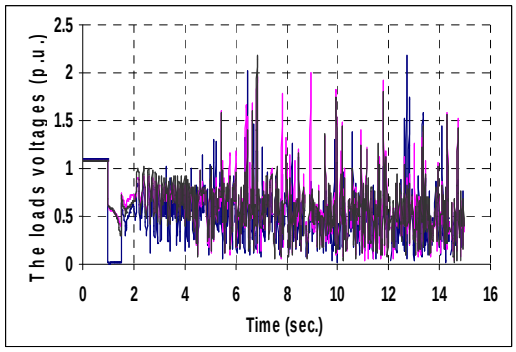

(d) V_S=1.1pu, CZ Loads, and T_C=576msec (h) V_S=1.1pu, CP Loads, and T_C=505msec

Fig. (6) Time response for loads voltages, 3-phase short-circuit, and load are considered as constant impedance, and constant power at node 4 with the GVM of generating units are (0.9p.u., and 1.1p.u.)

Figure (7) depicts the time response of load buses voltages, when the load bus (4) is an I.M. load (T=const.), while loads buses (5), and (6) are constant impedance loads. The GVM are taken as (0.9 p.u., and 1.1 p.u.). With (0.9 p.u.), voltages up to fault duration of 322 msec., the system voltage is stable, and when the fault duration of 323 msec., the system voltage starts to be unstable, as shown in figure 7 (a, b) respectively. For voltages of 1.1 p.u., when the fault duration is 495 msec., the system voltage is stable and when the fault duration is 496 msec., the system voltage become unstable, as shown in figure 6 (c, d) respectively. Also, figure 7 displays the time response of load buses voltages, when the load bus (4) is an I.M. load ($T \alpha \omega^2$) while loads buses (5), and (6) are constant impedance loads. The GVM adjusted to (0.9 p.u., 1.1 p.u. respectively). With GVM of (0.9 p.u.), the fault duration is 348 msec., the system voltage is stable, when the fault duration is 349 msec. the system voltage starts to be unstable, as shown in figure 7 (e, f) respectively. With GVM of (1.1 p.u.), the fault duration becomes 537 msec. the system voltage is stable. When the fault duration lasts to 538 msec., the system voltage will be unstable, as shown in figure 7 (g, h) respectively. Where: T_c refers to Fault Duration.

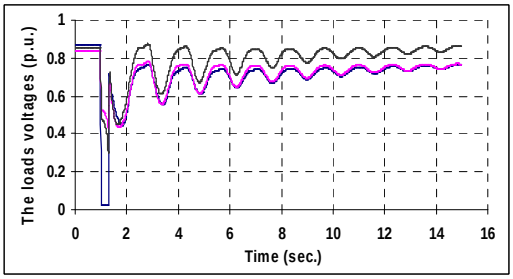

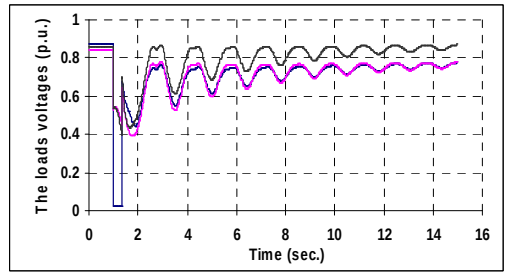

(a)V_S=0.9pu, IM, T=const loads, and T_C=322msec (e)V_S=0.9pu, IM $T\alpha\omega^2$loads, and T_C=348msec

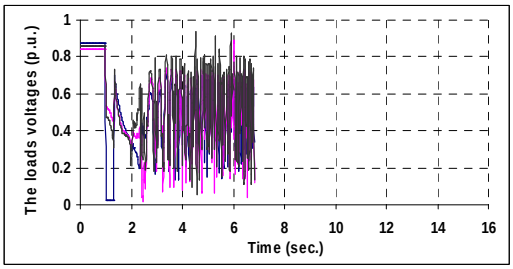

(b) V_S=0.9pu, IM (T=const.) Loads, and T_C=323msec

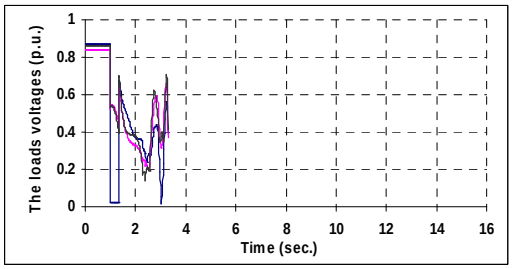

(f) V_S=0.9pu, ($T\alpha\omega^2$), and T_C=349msec

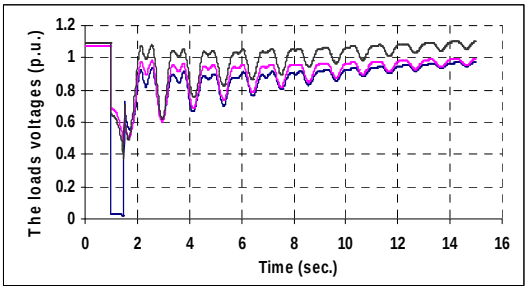

(c) V_S=1.1pu, IM (T=const.) Loads, and T_C=495msec

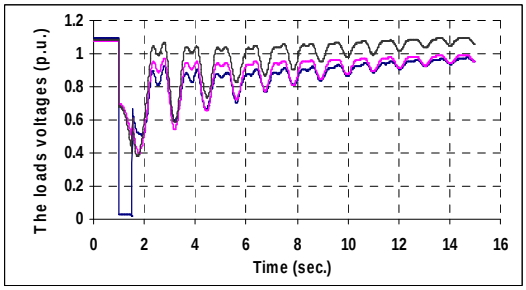

(g) V_S=1.1pu, ($T\alpha\omega^2$), and T_C=537msec

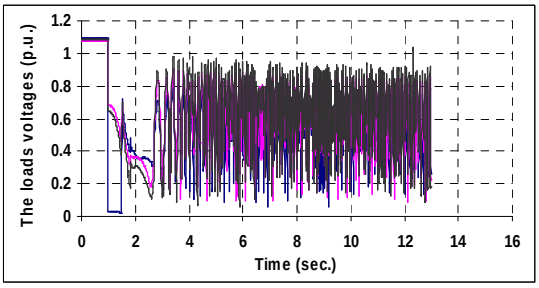

(d) V_S=1.1pu, IM (T=const.) Loads, and T_C=496msec

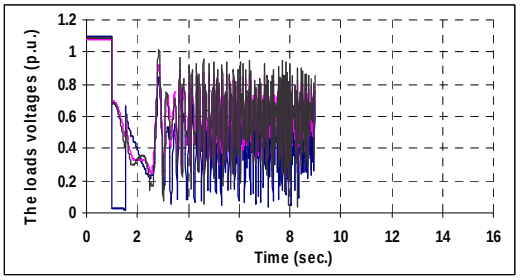

(h) V_S=1.1pu, ($T\alpha\omega^2$), and T_C=538msec

Fig. (7) Time response for loads voltages, 3-phase short-circuit, and loads are considered as I.M. load (T=const.), and I.M. load ($T\alpha\omega^2$) at node 4 with the GVM of generating units are 0.9p.u. and 1.1p.u.

4.4 Time response for loads voltages, with line opening, when the GVM of all generating units such as (0.90, 1.00, and 1.10) p.u.

The time response for load buses voltages at load buses with different values of the GVM of all generating units such as (0.90, 1.00, and 1.10) p.u., with constant impedance, and constant power loads are connected at all load buses, and I.M. load (T=const.), and I.M. load ($T\alpha\omega^2$) loads are connected at load bus (4) with the loads at load buses (5), and (6) are constant impedance loads, while the line between two buses (5) and (7) open at t=1 sec. Figure 8 (a, b, and c) indicates the time response for load buses voltages with the GVM are (0.90, 1.00, and 1.10) p.u. respectively, when the

loads connected at all load buses are constant impedance, and the GVM are 0.90 p.u., the fault duration required for voltage collapse equal 8.26 sec., when the GVM are 1.00 p.u., the fault duration required for voltage collapse equal 52.02sec., and when the GVM are 1.10 p.u., the fault duration required for voltage collapse is 213.56sec. While, the load connected at all load buses is constant power, and the GVM are 0.90 p.u., the fault duration which cause voltage collapse equal 0.94 sec., when the GVM are 1.00 p.u., the fault duration required for voltage collapse equal 12.48 sec., and when the GVM are 1.10 p.u., the fault duration which cause initiation of voltage collapse is 57.96 sec., as shown in figure 8 (d, e and f) respectively.

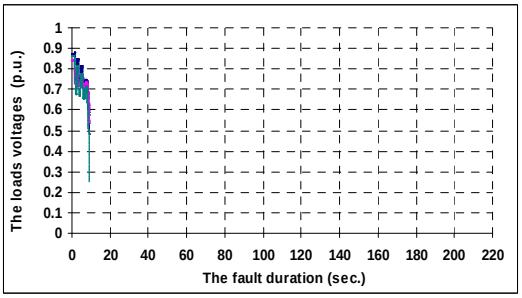

(a) V_S=0.9pu, CZ Loads, and T_C = 8.26 sec

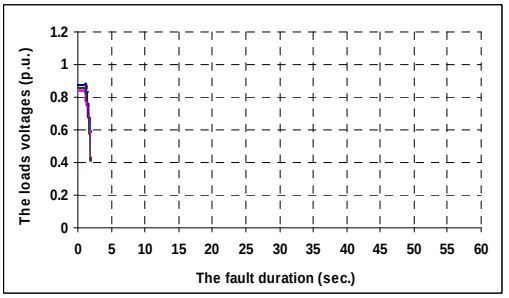

(d) V_S=0.9pu, CP Loads, and T_C = 0.94sec

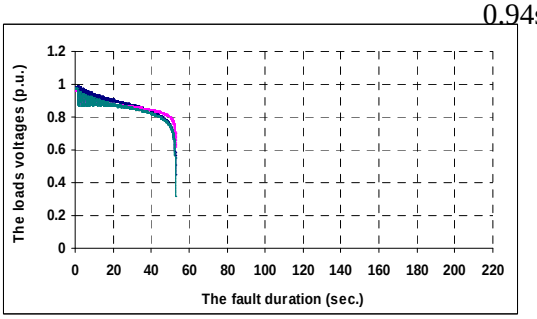

(b) V_S=1.0pu, CZ Loads, and T_C = 52.02 sec

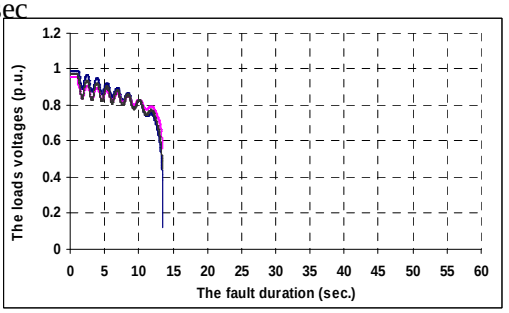

(e) V_S=1.0pu, CP Loads, and T_C = 12.48sec

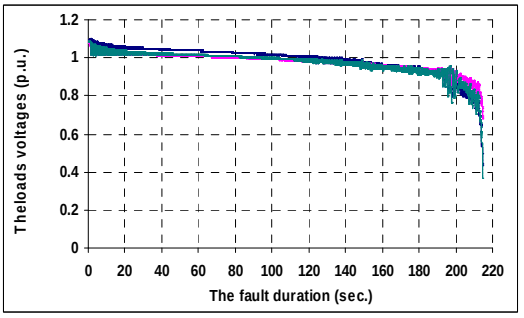

(c) V_S=1.1pu, CZ Loads, and T_C = 213.56 sec

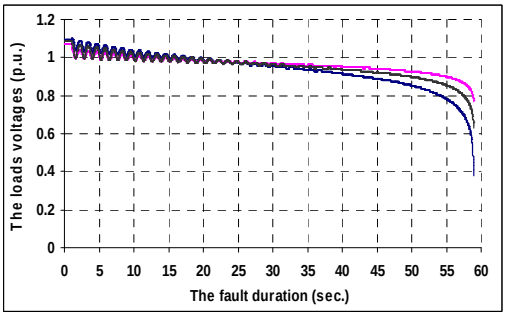

(f) V_S=1.1pu, CP Loads, and T_C = 57.96sec

Fig. (8) Time response for loads voltages, with line between nodes # 5 and # 7 opening with constant impedance, and constant power loads, and different values of the GVM (0.90, 1.00, and 1.10)p.u

Figure 9 (a, b and c) indicates that, the time response for load buses voltages when the load at load bus (4) is I.M. load (T=const.) with the loads at load buses (5), and (6) are constant impedance loads, with GVM of all generating units are (0.90, 1.00, and 1.10) p.u. respectively. With GVM of all generating units are (0.9 p.u.), the fault duration which cause voltage collapse equal 1.30 sec., when GVM are 1.00 p.u., the fault duration which cause voltage collapse equal 22.26 sec., and when GVM are 1.10 p.u., the fault duration which cause initiation of voltage collapse is 172.56 sec. While, the load at load bus (4) is I.M. load ($T \alpha \omega^2$) with the loads at load buses (5), and (6) are constant impedance loads. The GVM of all generating units are (0.9 p.u.). it is found that, the fault duration which cause voltage collapse occurrence is 4.16 sec., it is 30.22 sec. with GVM of 1.00 p.u., and 205.26 sec. with GVM are 1.10 p.u., as shown in figure 9 (d, e and f) respectively. Hence, from the figures, it is noticed that the fault duration which cause voltage collapse initiation increases by increasing the GVM of all generating units.

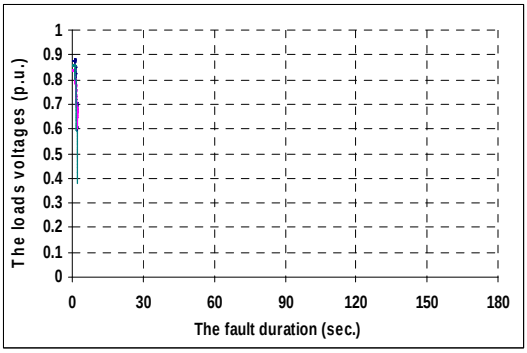

(a) V_S=0.9pu, IM T=const. loads, and T_C=1.3sec

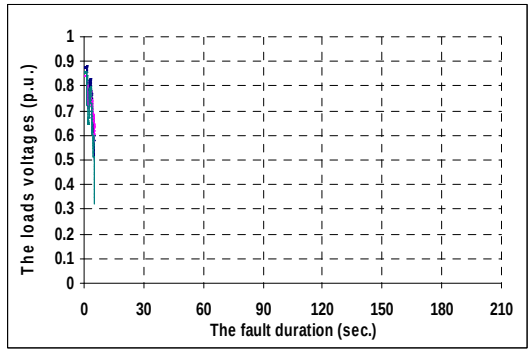

(d) V_S=0.9pu, IM $T\alpha\omega^2$ loads, and T_C=4.16sec

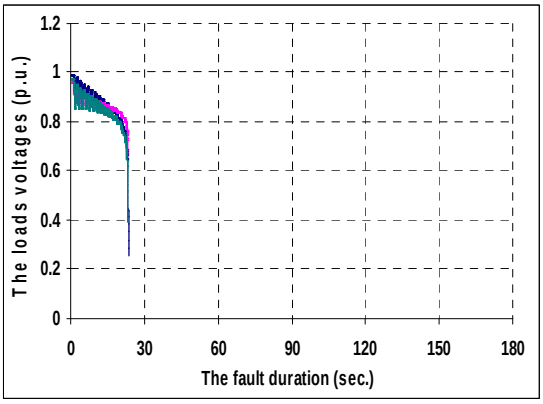

(b) V_S=1.0pu IM T=const. loads and T_C=22.26sec

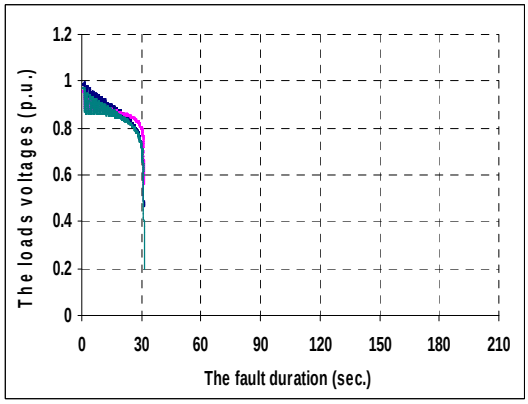

(e) V_S=1.0pu IM $T\alpha\omega^2$ loads, and T_C=30.22sec

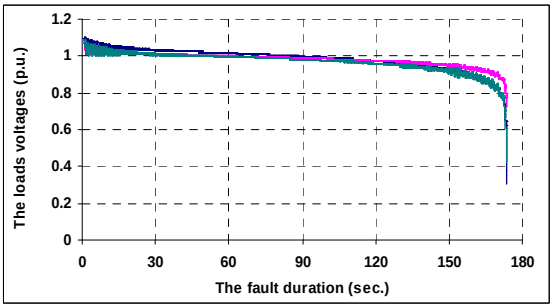

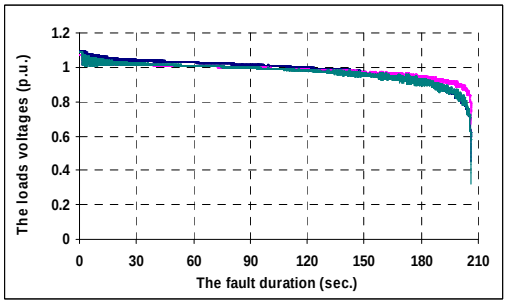

(c) V_S=1.1pu, IM T=const. loads and T_C=172.56sec (f) V_S=1.1pu IM $T\alpha\omega^2$ loads and T_C=205.26sec

Fig. (9) Time response for loads voltages, with line between nodes # 5 and # 7 opening with loads are considered as I.M. load (T=const.), and I.M. load ($T \alpha \omega^2$) at node (4), and different values of the GVM (0.90, 1.00, and 1.10)p.u

4.5 The polynomial Equation of Third Order:

The system is considered operating normally for 1sec. before fault is applied at nodes # 4 and # 5. The duration period which cause initiation of voltage instability in the considered system. The polynomial equation of third order which indicate the relation between fault duration which cause voltage instability with generators voltage magnitudes are:

(a) For Constant Impedance Loads at all load buses:

$$T_{Fault} = -4.1513 + 13.1961\,(GVM) - 13.5261\,(GVM)^2 + 4.9428\,(GVM)^3$$

(b) For Constant Current Loads at all load buses:

$$T_{Fault} = -9.1559 + 26.3536\,(GVM) - 24.9359\,(GVM)^2 + 8.1616\,(GVM)^3$$

(c) For Constant Power Loads at all load buses:

$$T_{Fault} = -9.9981 + 26.9855\,(GVM) - 24.0994\,(GVM)^2 + 7.5017\,(GVM)^3$$

(d) For I.M. load at node (4), nodes (5) and (6) are constant impedance loads:

for I.M. load (T=const.): $T_{Fault} = -2.9731 + 8.9478\,(GVM) - 8.6216\,(GVM)^2 + 3.0505\,(GVM)^3$

for I.M. load ($T\alpha\omega$): $T_{Fault} = -3.2467 + 9.8131\,(GVM) - 9.4908\,(GVM)^2 + 3.3401\,(GVM)^3$

for I.M. load ($T\alpha\omega^2$): $T_{Fault} = -4.9646 + 15.8790\,(GVM) - 16.4569\,(GVM)^2 + 5.9731\,(GVM)^3$

Also, the relation between fault duration which cause voltage collapse with generators voltage magnitudes.

(a) For Constant Impedance Loads at all load buses:

$$T_{Fault} = (1.039 - 3.1003\,(GVM) + 2.9936\,(GVM)^2 - 0.9247\,(GVM)^3) * 10^4$$

(b) For Constant Current Loads at all load buses:

$$T_{Fault} = (0.5299 - 1.4966\,(GVM) + 1.3385\,(GVM)^2 - 0.3674\,(GVM)^3) * 10^4$$

(c) For Constant Power Loads at all load buses:

$$T_{Fault} = 271.4749 - 205.9696\,(GVM) - 616.0938\,(GVM)^2 - 565.7239\,(GVM)^3$$

(d) For I.M. load at node (4), nodes (5) and (6) are constant impedance loads:

for I.M. load (T=const.): $T_{Fault} = (0.4557 - 1.2572\,(GVM) + 1.0828\,(GVM)^2 - 0.2774\,(GVM)^3) * 10^4$

for I.M. load (Tαω): T_{Fault}= *(0.8082 – 2.363 (GVM) + 2.2236 (GVM)^2 – 0.6636 (GVM)^3)*10^4*

for I.M. load (Tαω^2): T_{Fault}= *(0.873 – 2.5506 (GVM) + 2.3989 (GVM)^2 – 0.7158 (GVM)^3)*10^4*

Where T_{Fault} is measured by sec., and these equations have great error comparable with exact values of T_{Fault}.

6. CONCLUSIONS

A general formula for the allowed fault duration which cause initiation of voltage instability as a function in GVM is obtained, with different load types considered at system nodes. The fault duration which cause voltage instability increases by increasing the GVM of all generating units for each types of loads, when a 3-phase short-circuit occurs. When the load is constant impedance load connected at all load buses, the fault duration which cause voltage instability is greater than the fault duration which cause voltage instability when the load is constant current load, and both of them are greater than the fault duration which cause voltage instability when the load is constant power load. The induction motor load is connected at load bus (4), with the load at reminder load buses are constant impedance loads, when I.M. load type is (Tα ω^2), the fault duration which cause voltage instability is greater than the fault duration which cause voltage instability when I.M. load type is at (Tα ω), and both of them are greater than the fault duration which cause voltage instability when I.M. load type is (T= const.). A general formula for the allowed fault duration which causes voltage collapse initiation as a function in generators GVM is obtained, with different load types considered at system nodes. The fault duration which cause voltage collapse is influenced by the GVM of all generating units for each types of loads, with opening the transmission line between two nodes (5) and (7). Where, the fault duration which cause voltage collapse increases by increasing the GVM of all generating units. When the load is constant impedance load connected at all load buses, the fault duration which cause voltage collapse is greater than the fault duration which cause initiation of voltage collapse when the load is constant current load, and both of them are greater than the fault duration which cause voltage collapse when the load is constant power load. Also, when the induction motor load is connected at certain load bus, with the load at reminder load buses are constant impedance loads, when I.M. load type is (Tα ω^2), the fault duration which cause voltage collapse is greater than the fault duration which cause initiation of voltage collapse when I.M. load type is at (Tα ω), and both of them are greater than the fault duration which cause voltage collapse when I.M. load type is (T=const.).

REFERENCES

[1] M. Z. El-Sadek, “Power Systems Voltage stability”, Book, Muchtar Press, Assiut, Egypt, 2004.

[2] M. H. Haque, “Determination of Steady State Voltage Stability Limit Using P-Q Curve”, IEEE Power Engineering Review, pp. 71-72, April 2002.

[3] M. H. Haque, “Novel Method of Assessing Voltage Stability of A Power System Using Stability Boundary in P-Q Plane”, Electric Power Systems Research, Vol. 64, pp. 35-40, 2003.

[4] P. Kundur, "Power System Stability and Control", Book, Mc-Graw Hill, Inc, New York, USA, 1994.
[5] I. Musirin and T. K. Abdel-Rahman, "Estimating Maximum Loadability for Weak Bus Identification Using FVSI", IEEE, Power Engineering Review, pp. 50-52, November 2002.
[6] N. G. Abdel-Latif, "A Study on the Phenomenon of Voltage Instability in Electric Power Systems", M. Sc. Thesis, El-Minia University, Egypt, 2005.
[7] M. M. Hussien, "Fault Duration for Voltage Instabilities", M. Sc. Thesis, South Valley University, Egypt, 2006.
[8] P. A. Lõf, G. Anderson and D. J. Hill, "Voltage Stability Indices for Stressed Power Systems", IEEE Transactions on Power Systems, Vol. 8, No. 1, pp. 326-335, February 1993.
[9] P. Kessel and H. Glavitsch, "Estimating the Voltage Stability of A Power System" IEEE, Transactions on Power Delivery, Vol. PWRD-1, No. 3, pp. 346-354, July 1986.
[10] M. Charkravorty and D. Das, "Voltage Stability Analysis of Radial Distribution Networks", Electrical Power & Energy Systems, Vol. 23, pp. 129-135, 2001.
[11] M. Z. El-Sadek, "Preventive Measures for Voltage Collapses and Voltage Failures in the Egyptian Power System", Electric Power Systems Research Journal, No. 44, pp. 203-211, 1998.
[12] A. M. Hemeida, Y. A. Mobarak, M. M. Hussein, "Fault Duration for Voltage Instability and Voltage Collapse Initiation as Influenced by Load Window", International Review on Modeling and Simulations (I.RE.MO.S.), Praise Worthy Prize, Vol. 3, No. 5 pp. 911-917, October 2010.
[13] Cignatta, M.; Marannino, P.; Merlo, M.; Pozzi, M.; Zanellini, F.;" Load And Ltc Modeling For Voltage Stability Assessment In Ehv Network Studies", Power Tech, IEEE Russia, pp. 1 – 7, 2005.
[14] Helen Cheung, Lin Wang, Cungang Yang, "Network-Enabled Strategy And Platform For Corrective Actions Against Power System Instability", CCECE/CCGEI, Canada, pp. 1709-1714, 2008.
[15] F.A. Althowibi M.W. Mustafa, "Voltage Stability Calculations in Power Transmission Lines: Indications and Allocations", IEEE International Conference on Power and Energy (PECon), pp. 390 – 395, 2010.
[16] A.B.; Prada, R.B.; Da Guia da Silva, M.; "Voltage Stability Probabilistic Assessment in Composite Systems: Modeling Unsolvability and Controllability Loss Rodrigues Power Systems", IEEE Transactions on Power Delivery, Vol. 25, pp.1575 – 1588, 2010.
[17] Zhou, D.Q.; Annakkage, U.D.; Rajapakse, A.D.; "Online Monitoring of Voltage Stability Margin Using an Artificial Neural Network Power Systems ", IEEE Transactions on Power Delivery, Vol. 25, pp. 1566 – 1574, 2010.
[18] Xiaohua Huang; Guomin Zhang; Liye Xiao; "Optimal Location of SMES for Improving Power System Voltage Stability Applied Superconductivity", IEEE Transactions on Power Delivery, Vol. 20, pp. 1316 – 1319, 2010.
[19] Seethalekshmi, K.; Singh, S.N.; Srivastava, S.C.; "A Synchrophasor Assisted Frequency and Voltage Stability Based Load Shedding Scheme for Self-Healing of Power System Smart Grid", IEEE Transactions on Power Delivery, Vol. 2, pp. 221 – 230, 2011.

[20] Wiszniewski, A.; "New Criteria of Voltage Stability Margin for the Purpose of Load Shedding Power Delivery", IEEE Transactions on Power Delivery, Vol.22, pp. 1367 – 1371, 2007.

[21] Abdel-Akher, M.; Ahmad, M.E.; Mahanty, R.N.; Nor, K.M.; "An Approach to Determine a Pair of Power-Flow Solutions Related to the Voltage Stability of Unbalanced Three-Phase Networks Power Systems", IEEE Transactions on Power Delivery, Vol. 23, pp.1249 – 1257, 2008.

[22] Yunfei Wang; Pordanjani, I.R.; Weixing Li; Wilsun Xu; Tongwen Chen; Vaahedi, E.; Gurney, J.; "Voltage Stability Monitoring Based on the Concept of Coupled Single-Port Circuit Power Systems", IEEE Transactions on Power Delivery, Vol. 26, pp. 2154 – 2163, 2011.

[23] Leonardi, B.; Ajjarapu, V.; "Development of Multilinear Regression Models for Online Voltage Stability Margin Estimation Power Systems", IEEE Transactions on Power Delivery, Vol. 26, pp. 374 – 383, 2011.

[24] Feng Dong; Chowdhury, B.H.; Crow, M.L.; Acar, L.; "Improving voltage stability by reactive power reserve management Power Systems", IEEE Transactions on Power Delivery, Vol.20, pp.338-345, 2005.

[25] Du, W.; Chen, Z.; Wang, H.F.; Dunn, R.; "Feasibility of online collaborative voltage stability control of power systems Generation", Transmission & Distribution, IET Vol.3, pp. 216 – 224, 2009.

APPENDIX

System Differential Equations:

$$[g([x],[y])]=0 \tag{1}$$

$$\left[\dot{y}\right]=[f([x],[y])] \tag{2}$$

Network General Features:

$$\begin{bmatrix} I_G \\ V_L \end{bmatrix}=\begin{bmatrix} Y_{GG} & K_{GL} \\ H_{LG} & Z_{LL} \end{bmatrix}\begin{bmatrix} V_G \\ I_L \end{bmatrix} \tag{3}$$

$$\begin{bmatrix} V_Q \\ V_D \end{bmatrix}=\begin{bmatrix} \cos\theta & -\sin\theta \\ \sin\theta & \cos\theta \end{bmatrix}\begin{bmatrix} v_q \\ v_d \end{bmatrix} \tag{4}$$

$$\begin{bmatrix} v_q \\ v_d \end{bmatrix}=\begin{bmatrix} \cos\theta & \sin\theta \\ -\sin\theta & \cos\theta \end{bmatrix}\begin{bmatrix} V_Q \\ V_D \end{bmatrix} \tag{5}$$

Steady-state equations solution:

$$\begin{bmatrix} v_q \\ v_d \end{bmatrix}=\begin{bmatrix} E_q^{'} \\ E_d^{'} \end{bmatrix}-\begin{bmatrix} R_a & -x_d^{'} \\ x_q^{'} & R_a \end{bmatrix}\begin{bmatrix} I_q \\ I_d \end{bmatrix} \tag{6}$$

$$I = I_{real} + jI_{imag}\text{, and } I_q + jI_d = Ie^{-j\theta} \tag{7}$$

$$v_q + jv_d = \left(E_q^{'} + jE_d^{'}\right) - \left(R_a + jx_d^{'}\right)\left(I_q + jI_d\right) \tag{8}$$

$$V = E^{/} - \left(R_a + jx_d^{'}\right)I \tag{9}$$

$$\begin{bmatrix} V_{real} \\ V_{imag} \end{bmatrix} = \begin{bmatrix} E_{real}^{'} \\ E_{imag}^{'} \end{bmatrix} - \begin{bmatrix} \cos\theta & -\sin\theta \\ \sin\theta & \cos\theta \end{bmatrix} \begin{bmatrix} R_a & -x_d^{'} \\ x_q^{'} & R_a \end{bmatrix} \begin{bmatrix} \cos\theta & \sin\theta \\ -\sin\theta & \cos\theta \end{bmatrix} \begin{bmatrix} I_{real} \\ I_{imag} \end{bmatrix} \tag{10}$$

$$Y^{fict} = \frac{R_a - j\frac{1}{2}\left(x_d^{'} + x_q^{'}\right)}{R_a^2 + x_d^{'}x_q^{'}} \tag{11}$$

$$E^{fict} = E^{/} + \frac{j\frac{1}{2}\left(x_q^{'} - x_d^{'}\right)}{R_a - j\frac{1}{2}\left(x_d^{'} + x_q^{'}\right)}\left(E^{/*} - V^{*}\right)e^{j2\theta} \tag{12}$$

$$\begin{bmatrix} I_G \\ I_L \\ 0 \end{bmatrix} = \begin{bmatrix} Y_{GG} & Y_{GL} & Y_{GR} \\ Y_{LG} & Y_{LL} & Y_{LR} \\ Y_{RG} & Y_{RL} & Y_{RR} \end{bmatrix} \begin{bmatrix} E^{fict} \\ V_L \\ V_R \end{bmatrix} \tag{13}$$

$$\begin{bmatrix} I_G \\ V_L \end{bmatrix} = \begin{bmatrix} Y & H \\ K & Z \end{bmatrix} \begin{bmatrix} E^{fict} \\ I_L \end{bmatrix} \tag{14}$$

عدم أتزان الجهود وضمور الجهود نتيجة تأثير قيم جهود المولدات الفترات الزمنية اللازمة لإحداث

البحث يحدد الفترة الزمنية اللازمة التي يستغرقها العطل لإحداث عدم إتزان الجهود وإما ضمور الجهد إلى قيم متدنية يصعب معها استمرار الأحمال في العمل حيث أن كلا الظاهرتين تؤديان في الغالب إلى الإطفاء التام للشبكة الكهربية وذلك بتأثير قيم جهود المولدات على الفترة الزمنية اللازمة لإحداث ظاهرتي عدم إتزان الجهود وضمور الجهود. ويحدد البحث الحدود الزمنية التي تفصل بين إتزان الجهود وعدمها وبين ضمور الجهود وعدمها فضلا عن معادلات للفترة الزمنية مع قيم جهود المولدات في صورة متوالية عددية.